

The response of river discharge to climate fluctuations in the source region of the Yellow River

Jianfeng Zhang · Guomin Li · S. Liang

Received: 24 July 2010 / Accepted: 30 September 2011 / Published online: 14 October 2011
© Springer-Verlag 2011

Abstract The Yellow River is the second biggest river in China and serves as a source of domestic and agricultural water supply in the watershed. In the last several decades, this river's discharge reduced to zero several times since 1960, especially in the 1990s. The decreasing river flow has caused some serious eco-environmental problems in the source region. To study the important effects of climate on river discharge in the source area, a data set of 44 water-year river flow, air temperature and precipitation is selected and wavelet analysis is performed to describe and identify the features of climate (air temperature and precipitation) and river discharge. Results of continuous wavelet transform (CWT) show that all three parameters have common significant periods of 1–2 and 3–6 years against red noise in different time spans while river discharge probably has a 16-year-period mainly in the cone of influence (COI). Comparison of river flow and its CWT suggests these zero river flows are connected to extreme low values located in different scales, indicating that climate does control the river discharge in the source area. The cross wavelet (XWT) and wavelet coherence (WTC) clearly illustrate that the first zero river discharge (about in 1961) is only

related to precipitation, while the rest have resulted from the combination of air temperature and precipitation.

Keywords The Yellow River · Zero discharge · Cross wavelet · Wavelet coherence

Introduction

Water resource is essential for the living and development of the human race. As the source of several big Asian rivers, Tibet Plateau is called “the first water tower in the Asia” (Li 2000). The Yellow River is one of those rivers and is also important for water supply in northwestern and northern China because it flows across eight provinces from the west to the east before reaching the Bohai Sea (Fig. 1). According to the Yellow River Commission (1999), the river is the second biggest in China, 5,464 km long, with an area of 752,443 km² hosting 30% of China's population.

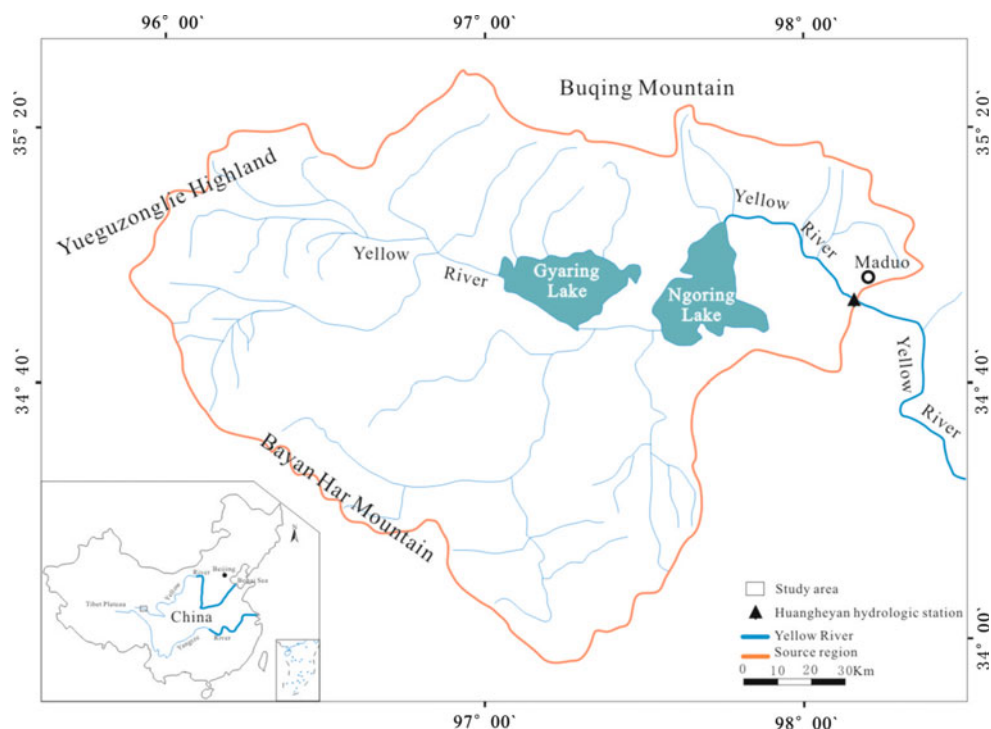
In the background of global warming (IPCC 1996, 2001 and 2007), the upper reaches of the Yellow River has suffered zero discharge several times since 1960, resulting in serious eco-environmental problems, such as grassland degradation, shrinking lake water area and soil desertification, in the source region (Chen et al. 1998). Some researchers insisted that eco-environment degradation in the source region was caused by human activities, especially continuous grazing (Zhang et al. 2006; Bai et al. 2002; Yan et al. 2003). But Fu et al. (2004) revealed that the runoff of the watershed had decreased even after human uses were forbidden. Because climatic variables, such as temperature and precipitation, may also have strong influences on ecosystems, some studies suggested that the problems were owing to increasingly dry and warm climate

J. Zhang · G. Li
Division of Engineering Geology and Water Resources,
Institute of Geology and Geophysics, Chinese Academy
of Sciences, Beijing 100029, China

J. Zhang (✉)
Graduate University of Chinese Academy of Science,
Beijing, China
e-mail: zhangjianfeng@mail.iggcas.ac.cn

S. Liang
School of Water Resources and Environment,
China University of Geosciences, Beijing 100083, China

Fig. 1 Location of the Yellow River and its source region (the figure is done in CoreDraw X3)



(Karl et al. 1995; Boo et al. 2004). A few studies have shown that precipitation in arid and semi-arid zone was significantly affected by the climbing temperature (Hess et al. 1995; Elagib and Abdu 1997; Modarres and da Silva 2007). Zhang et al. (2004) suggested that the Yellow River source region had a negative water budget since 1990 due to increasing temperatures and reducing runoff from highlands. Existing qualitative analysis on the mechanics of these zero river discharges showed that the zero river discharge around 1980 resulted from the combination of temperature and precipitation, but the physical reasons for the rest zero river discharges have not been presented (Liang et al. 2010). To date, the causes for dry-up of the Yellow River in its source region is still unclear.

Generally, spectral analyses (Fourier transform) are frequently used to investigate frequency component of time series, and correlation function is used to explore the relationship between different parameters (Chatfield 1980; Huang 1983; Chen 1988). With the development of wavelet analysis, many researchers have used it to analyze the component of time series, for its character of time–frequency localization (Smith et al. 1998; Andreo et al. 2006; Rossi et al. 2009). Subsequently, cross wavelet and wavelet coherence were brought forward (Liu 1994; Torrence and Compo 1998). Cross wavelet is aimed at revealing the correlations between two series at different frequencies and time locations, and wavelet coherence indicates how well one parameter corresponds to the other. And the tool has also been used to study the relationship between Arctic Oscillation (AO) and maximum annual ice

extent in the Baltic Sea (BMI) (Grinsted et al. 2004). Thereafter, the wavelet analysis is frequently used in meteorology (Moore et al. 2006; Yang et al. 2010) and hydrology (Schaeffli et al. 2007; Labat 2010).

Although Liang et al. (2010) has deeply analyzed the characteristics of the river discharge, analyses on the detailed correlations between climate factors and river discharge in the source region of the Yellow River were not performed. This study is aimed to quantitatively describe the characteristics of climatic factors and river discharge, and examine the inner relations between discharge and climate factors.

The study area and data

The Yellow River source region is bounded by the Buqing Mountain in the north, the Bayan Har Mountain in the south, and the Yueguzonglie highland in the west, with an area of 20,930 km² (Fig. 1). Its relief falls from northwest to southeast with elevation from 5,270 to 4,000 m a.s.l., and most of the region is above 3,000 m. There were about 5,300 lakes in the region in the 1980s, but many of them had shrunk or disappeared in the last two decades. Two most important lakes in this region are the Gyaring Lake and the Ngoring Lake, with water areas of 526 and 611 km², respectively. The Yellow River flows through the two lakes and by the Huangheyan hydrologic station.

Climate of the study area is characterized by cold and semi-arid or semi-humid alpine style, with an annual mean

air temperature of -4.0 to 1.1°C . The annual precipitation ranges from 300 to 750 mm, 75% of which occurring from June to September. The potential evaporation capability is $1,300$ – $1,400$ mm/year, and the vegetation season lasts from May to September (Liang et al. 2010).

The semi-yearly average time series are selected in the paper. River discharge data used for analysis is collected from the Huangheyuan hydrologic station and air temperature and precipitation data from the Maduo Meteorological Station (Fig. 1). The time series covers a span of 44 water-years, from 1955 to 1998. The first hydrological station in the river’s source region is Huangheyuan hydrologic station, which started running in 1955, but stopped during 1968 and 1975 for some reason. The annual river discharge fluctuates between 0.07×10^8 in 1979 and $25.85 \times 10^8 \text{ m}^3$ in 1975, with an average of $4.41 \times 10^8 \text{ m}^3$ per year (Fig. 2c). The time span in this study remains representative of the studied phenomena (zero river discharge). Zero river discharges in the source region has occurred four times over the time range in the recorded history: 10 December 1960 to 17 March 1961; 19 December 1979 to 10 March 1980; 2 February to 29 February 1996 and 1 January to 28 February 1998. The missing data from 1968 to 1975 is calculated by linear interpolation using the data from the closest station at Jimai which is 270 km downstream of the Huangheyuan hydrologic station (Liang et al. 2010).

Methods

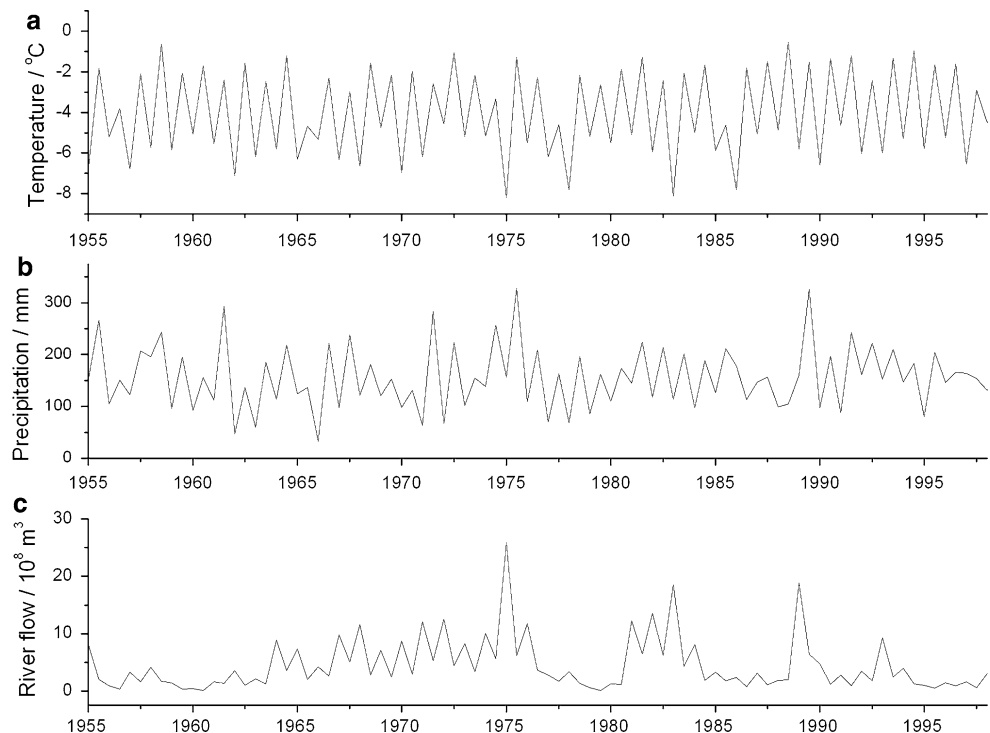
The wavelet transform is a time–frequency decomposition based on wavelet functions localized in both time and frequency (Daubechies 1990). Contrary to the Fourier transform, the wavelet transform decomposes one signal into a sum of wave functions with finite length in order to maintain the time localization of frequencies. A reference wavelet function $\psi(t)$ is called “mother wavelet”, and it produces a set of functions after translation and dilation, called “daughter wavelets” with scale parameter a and time localization parameter b :

$$\psi_{a,b}(t) = \frac{1}{\sqrt{a}} \cdot \psi\left(\frac{t-b}{a}\right). \tag{1}$$

Parameter a will vary during transform and is used to investigate different frequency levels or periodicities, while parameter b is for translation of the daughter wavelet on the time axis to detect the presence of a given frequency at any time. To be “admissible” as a wavelet, the wavelet must have a zero mean and be localized in both time and frequency space (Farge 1992).

Morlet wavelet is selected since it provides a good balance between time and frequency localization (Grinsted et al. 2004) and a good choice for feature extraction. The Morlet wavelet consists of a plane wave modulated by a Gaussian:

Fig. 2 Semiannual records of **a** air temperature, **b** precipitation and **c** river flow, from 1955 to 1998 (the figure is done in OriginPro 7.5)



$$\psi(\eta) = \pi^{-1/4} e^{i\omega_0\eta} e^{-\eta^2/2} \quad (2)$$

where ω_0 is the non-dimensional frequency, here taken to be 6. For Morlet wavelet (with $\omega_0 = 6$), the Fourier period is almost equal to the scale. The continuous wavelet transform (CWT) of a time series x_n ($n = 1, 2, \dots, N$) with uniform time steps δt , is defined as the convolution of x_n with scaled and normalized wavelet:

$$W_n^X(s) = \sqrt{\frac{\delta t}{s}} \sum_{n'=1}^N x_{n'} \Psi \left[(n' - n) \frac{\delta t}{s} \right] \quad (3)$$

CWT can be performed in Fourier space using a discrete Fourier transform (Torrence and Compo 1998). The complex argument of $W_n^X(s)$ can be interpreted as the phases of $X\{\phi_1 \dots \phi_n\}$. The wavelet power is defined as $|W_n^X(s)|^2$.

Because of padding with zeroes at the end of the time series before doing the CWT, discontinuities are introduced at the endpoints and the amplitude near the edges decreases. The cone of influence (COI) is the region where edge effects become important and the wavelet power caused by discontinuity has dropped to e^{-2} of the value at the edge.

Many geophysical time series have distinctive red noise characteristics modeled by a first order autoregressive (AR1) process. The Fourier power spectrum of an AR1 process with lag-1 autocorrelation α (Allen and Smith 1996) is given by:

$$P_k = \frac{1 - \alpha^2}{|1 - \alpha e^{-2i\pi k}|^2} \quad (4)$$

where k is the Fourier frequency index.

The cross wavelet (XWT) transform of two time series X and Y is defined as $W^{XY} = W^X W^{Y*}$ by Torrence and Compo (1998), where $*$ denotes complex conjugation. We further define the XWT power as $|W^{XY}|$, which signifies areas with high common power and reveals inherent phase relationship. If the two series are physically related, we would expect a consistent or slowly varying phase lag (Grinsted et al. 2004). The complex argument $\arg(W^{XY})$ can be interpreted as the local relative phase between X and Y in the time frequency space. The distribution of the XWT power of two time series with background power spectra P_k^X and P_k^Y is given by Torrence and Compo (1998)

$$D \left(\frac{|W^X W^{Y*}|}{\sigma_X \sigma_Y} < p \right) = \frac{Z_v(p)}{v} \sqrt{P_k^X P_k^Y} \quad (5)$$

where $Z_v(p)$ is the confidence level associated with the probability p for a probability distribution function (PDF) defined by the square root of the product of two χ^2 distributions. σ_X and σ_Y are the variances of time series X and Y , respectively. The 5% significance level is calculated using $Z_2(95\%) = 3.999$.

The wavelet coherence (WTC) is used to measure coherence of the cross wavelet transform in time–frequency space and Torrence and Webster (1999) have defined the wavelet coherence of two time series as:

$$R_n^2(s) = \frac{|S(s^{-1} W_n^{XY}(s))|^2}{S(s^{-1} |W_n^X(s)|^2) \cdot S(s^{-1} |W_n^Y(s)|^2)} \quad (6)$$

where S is a smoothing operator which is a Gaussian along the time axis and boxcar along the wavelet scale axis, and designed to fit the wavelet decor relation length. Noticing the definition of WTC closely resembles that of a traditional correlation coefficient, it is useful to consider it as a localized correlation coefficient in time frequency space. The Monte Carlo method is used to test significance with a red noise model (Grinsted et al. 2004).

Results

Features of river discharge and climate factors

The CWT power spectrums with 5% significant level against red noise for river discharge, precipitation and air temperature are shown in Fig. 3. For river discharge (Fig. 3a), wavelet power distribution is completely limited. Periodicity is only significant in the band of about 3–6 years between 1972 and 1988. And there are other periods in the band of 1–2 years during 1970–1978 and 1988–1992, with 20% significance level against red noise (not shown here). However, there may be a persistent and significant period around the period of 16 years throughout the time range (1955–1998) although mainly located in the COI. Precipitation shows some similar patterns of the wavelet power spectrum as river discharge (Fig. 3b), except that precipitation has a significant period in the band of 1–2 years during 1956–1976 and 1988–1991, with 5% significance level against red noise, and no apparent fluctuation in the band above 16 years where the edge effects become considerable. Most of the power is concentrated within the band of about 1–6 years. A period of 3–6 years is significant from about 1967 to 1987, which also presents in the river discharge but has a time advance. Unlike river discharge and precipitation in the source region, the air temperature (Fig. 3c) only shows two periods: 1971–1991, with a significant period of 1–2 years against red noise, and a period of 3–6 years in the band of 1964–1988 with an obvious shift from a period of about 5 years to a shorter period of 4 years. The shift of period indicates that temperature changes more frequently in the time late.

Fig. 3 Wavelet power spectrum of **a** river flow, **b** precipitation and **c** temperature. The thick black contour designates 5% significance level against red noise. The *bottom axis* is time and the *left axis* is period equivalent to that in the Fourier transform. The cone of influence (COI) where edge effects become important is indicated as lighter shadings (the figure is done in Matlat 6.5)

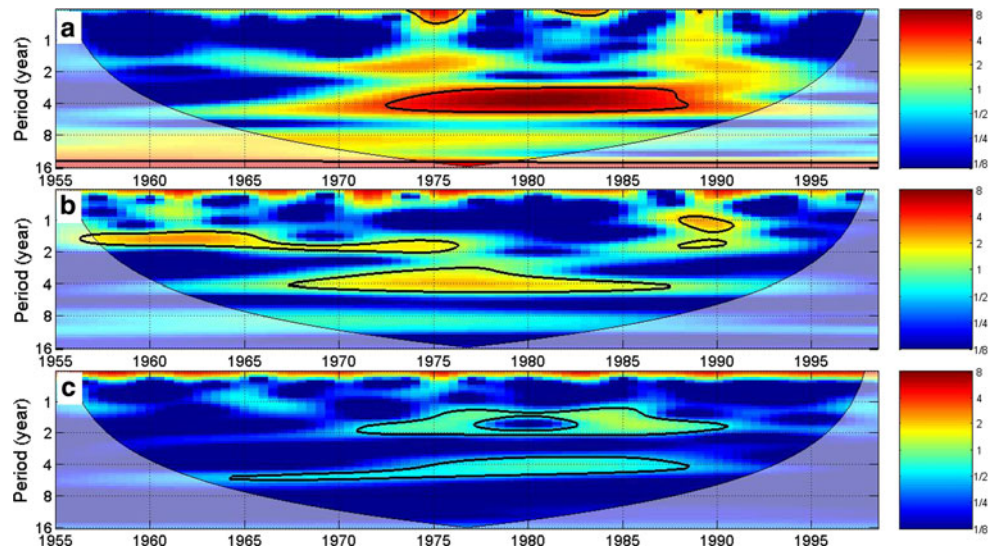
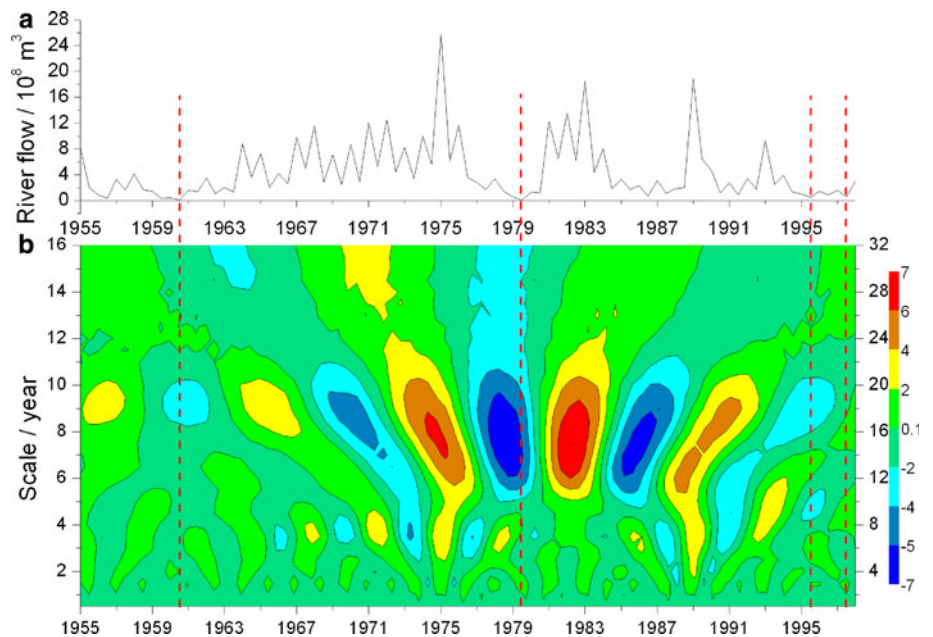


Fig. 4 The real part of wavelet coefficients of river flow (**b**) and the plot of semiannual river flow (**a**). The *vertical dashed red lines* indicate zero flows of the river in the history of record (the figure is done in Matlat 6.5)



To describe the characteristics of the zero river discharges in the history record, the real part of the wavelet coefficients of river discharge is plotted in Fig. 4b together with the river discharge records (Fig. 4a). It is obviously shown that each zero river discharge corresponds to low wavelet coefficients of a certain scale. Among the four zero river discharges, the first one (around 1961) is likely to correlate with the scale of 5–10 years, and the zero around 1980 correlates with the band of about 8 years, while the last two zero discharges (the early 1996 and 1998) are probably corresponding to scales of 5 and 9 years. Based on these understandings of time–frequency features of these zero river flows, the relationship between discharge and climatic factors could be analyzed by XWT and WTC.

Relationship: cross wavelet

According to the features of precipitation, air temperature and river discharge suggested in the CWTs, some common properties can be summarized in the wavelet power of the three time series, such as a peak in the ~4 years band around 1980. However, the similarity showed in periods here is quite low and it is therefore hard to discern if it is merely a coincidence. The XWT makes sense in this regard as it reveals areas with high common power between two time series.

The cross wavelet power (XWT) of river discharge versus precipitation is shown in Fig. 5a. The common features of individual wavelet transforms (Fig. 3a, b) can

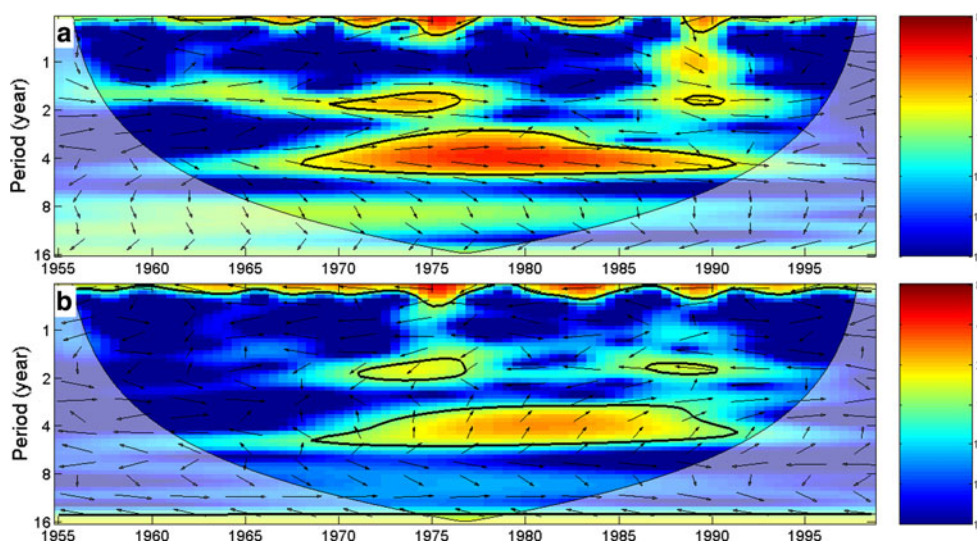


Fig. 5 Cross-wavelet transform (XWT) of river flow-precipitation (**a**) and river flow-temperature (**b**). The *thick black contour* means 5% significance level against red noise. The relative phase relationship is shown as *arrows* (with in-phase pointing *right*, anti-phase pointing *left*, and river flow leading precipitation or temperature by 90°

pointing straight up, and the vice versa). The *bottom axis* is time and the *left axis* is period equivalent to that in the Fourier transform. The cone of influence (COI) where edge effects become important is indicated as *lighter shadings* (the figure is done in Matlab 6.5)

be easily distinguished with the significant level of 5%. There are significant common powers in the 1- to 2-year band during both 1967–1977 and 1988–1992, and the band of 3–6 years from 1973 to 1988. For there to be a simple cause and effect relationship between river discharge and precipitation, a locked phase between the two variables will be expected. In fact, almost all the arrows, which indicate phase between two series, point right. Cross wavelet power shows that the river discharge and precipitation are in phase at all the significant common power area, suggesting the positive correlation between river discharge and precipitation. However, the phase at specific scale is predominantly consistent even outside the significant power area, indicating a stronger link for phase than results implied by the XWT spectrum between river discharge and precipitation.

Similar to the XWT of river discharge and precipitation, the XWT between river discharge and temperature (Fig. 5b) also shows common power in the band of 3–6 years from 1967 to 1992 and 1–2 years band over both 1968–1977 and 1985–1991, whereas it is mainly anti-phase in the band of 1–2 years, and slightly shifts to the place where the river discharge leads temperature by about 1.05 rad in the period of 3–6 years. Additionally, a band of about 16 years is also significant with a phase of about 2.6 rad, but most part falls in the COI.

Relationship: wavelet coherence

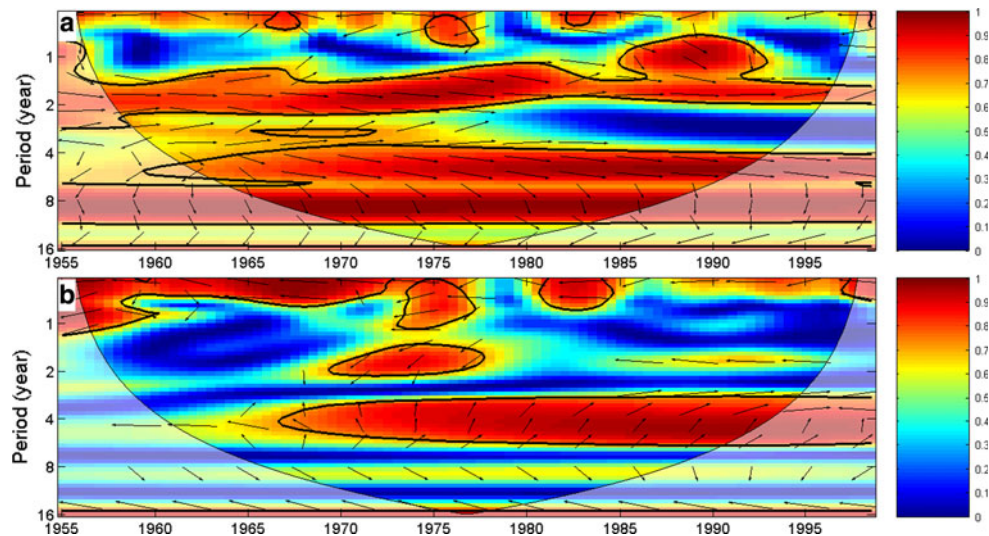
Figure 6 shows the WTC between river discharge and climate factors. Compared with XWT, there is a larger area

of WTC of river discharge and precipitation (Fig. 6a) as being significant against red background noise with 5% significant level. This result basically shows a consistent in-phase relationship in the periods of 1–2 and 4–6 years throughout the investigating period, implying a positive correlation (Girardin et al. 2006) between river discharge and precipitation. When it goes to a longer period (or larger scale), e.g. 6–10 years, the arrow is slowly shifted down. Therefore, it can be concluded that the river discharge in the source region varies closely with precipitation in the periods of 1–2 and 4–6 years. Unlike the correlation pattern of discharge and precipitation, WTC of river discharge and temperature shows a large area being significant in the bands of 3–6 from 1967 to 1998 and 1–2 years from 1968 to 1977 (Fig. 6b), which reveals a consistent relationship in the significant bands between the two variables.

Discussion and conclusion

The time–frequency properties of river discharge, air temperature and precipitation were summarized using wavelet analysis. The CWT indicates almost identical significant periods of 3–6 and 1–2 years for all the three time series but in different time ranges. As for temperature in the period of 3–6 years, a notable shift toward a smaller scale is presented about in 1975, meaning a more frequent fluctuation for temperature at the point of time in the source region. Comparison between the discharge and its real coefficients of CWT reveals that each zero river discharge is corresponding to a certain scale.

Fig. 6 Squared wavelet coherence (WTC) between river flow and precipitation (a) and river flow and temperature (b). The 5% significance level against red noise is shown as a *thick black contour*. Arrows indicate the phase shift (pointing *right* means in phase, pointing *left* anti-phase and pointing *straight up* is that the river flow leads precipitation or temperature by 90°). The *bottom axis* is time and the *left axis* is period equivalent to that in the Fourier transform. The cone of influence (COI) where edge effects become important is indicated as *lighter shadings* (the figure is done in Matlat 6.5)



The XWT of river discharge and precipitation shows a significant power in the band of 3–6 years from 1967–1992, during which the 1980s zero river discharge occurred. All scales with significant common power are in phase in the XWT. The XWT of river discharge and temperature also presents a great power and consistent phase in the 3- to 6-year band from 1967 to 1992. Therefore, these results mean that the second zero river discharge is related most likely to both precipitation and temperature.

The WTC between river discharge and precipitation shows a significant coherence and a consistent in-phase relationship in the band of 4–10 years throughout the record time span. Because all the four zero river discharges occurred within the band of period, it can be inferred that they are all ascribed to precipitation. Differently, the WTC between river discharge and temperature only shows consistent phase relationship in the bands of 3–6 years from 1967 to 1998 and 1–2 years from 1967 to 1998 and 1968–1977, indicating the first zero river discharge is not related to temperature whilst the rest are correlated with temperature.

The periodicity results of river discharges and climate factors illustrated in this paper are somewhat different from the conclusion drawn by Liang et al. (2010). Without significant test, they concluded that there were 7–8 and 3–4 year periods by visual observation in river discharge, precipitation and air temperature and attributed the 1980s zero discharges to precipitation and high temperature while the other zero discharges to precipitation. The discrepancy is likely caused by their grounding on some whole scale (coefficients at some whole scales) instead of localization of wavelet analysis. XWTs and WTCs analyses have shown that the first zero discharge (from the late 1960 to the early 1961) may have just resulted from the low precipitation in the source region, while the other zero river discharges are likely to be the result of a combination of precipitation and temperature in the source region.

Acknowledgments We thank the two anonymous reviewers for their valuable comments and suggestions. This research was supported by the Knowledge Innovation Program of the Chinese Academy of Sciences (KZCX2-YW-Q06-2-3), the National Natural Science Foundation of China (No. 41072187), and the High-level Radioactive Waste Geological Disposal Project from State Administration of Science Technology and Industry for National Defense.

References

Allen MR, Smith LA (1996) Monte Carlo SSA: detecting irregular oscillations in the presence of colored noise. *J Climate* 9(12):3373–3404

Andreo B, Jimenez P, Duran JJ, Carrasco F, Vadillo I, Mangin A (2006) Climatic and hydrological variations during the last 117–166 years in the south of the Iberian Peninsula, from spectral and correlation analyses and continuous wavelet analyses. *J Hydrol* 324(1–4):24–39

Bai W, Zhang Y, Xie G, Shen Z (2002) Analysis formation causes of grassland degradation in Madoo County in the source region of Yellow River. *Chin J Appl Ecol* 13(7):823–826 (in Chinese)

Boo KO, Kwon WT, Kim JK (2004) Vegetation change I the regional surface climate over East Asia due to global warming using BIOME4. *Geophys Space Phys* 27:317–327

Chatfield C (1980) *The analysis of time series: an introduction*, 2nd edn. Chapman and Hall, London

Chen B (1988) *Groundwater dynamics and its forecasting*. Science Press, Beijing (in Chinese)

Chen Q, Liang Q, Wei Y (1998) Study on degraded rangelands in Darlag county of Qinghai Province. *J Pratacult Sci* 7(4):44–48

Daubechies I (1990) The wavelet transform, time–frequency localization and signal analysis. *IEEE Trans Inf Theory* 36(5):961–1005

Elagib NA, Abdu ASA (1997) Climate variability and aridity in Bahrain. *J Arid Environ* 36(3):405–419

Farge M (1992) Wavelet transforms and their applications to turbulence. *Annu Rev Fluid Mech* 24:395–457

Fu GB, Chen SL, Liu CM, Shepard D (2004) Hydro-climatic trends of the Yellow River basin for the last 50 years. *Climatic Change* 65(1–2):149–178

Grinsted A, Moore JC, Jevrejeva S (2004) Application of the cross wavelet transform and wavelet coherence to geophysical time series. *Nonlinear Process Geophys* 11(5–6):561–566

- Hess TM, Stephens W, Maryah UM (1995) Rainfall trends in the north-east arid zone of Nigeria 1961–1990. *Agric For Meteorol* 74(1–2):87–97
- Huang Z (1983) *Spectral analysis and its application to hydrometeorology*. China Meteorological Press, Beijing
- IPCC (1996) *Climate change 1995: impacts, adaptation, and mitigation*. Cambridge University Press, Cambridge
- IPCC (2001) *Climate change 2000: impacts, adaptation, and vulnerability*. Cambridge University Press, Cambridge
- Karl TR, Knight RW, Plummer N (1995) Trends in the high-frequency climate variability in the twentieth century. *Nature* 377:217–220
- Labat D (2010) Cross wavelet analyses of annual continental freshwater discharge and selected climate indices. *J Hydrol* 385(1–4):269–278
- Li W (2000) Review and expectation in study of hydrology and water resource of the Yellow River source region in the 20th century. *J Qinghai Univ* 18:50–53 (in Chinese)
- Liang S, Ge S, Wan L, Zhang J (2010) Can climate change cause the Yellow River to dry up? *Water Resour Res* 46
- Liu PC (1994) Wavelet spectrum analysis and ocean wind waves. In: *Wavelets in geophysics*. Academic Press, Beijing, pp 151–166
- Modarres R, da Silva VDR (2007) Rainfall trends in arid and semi-arid regions of Iran. *J Arid Environ* 70(2):344–355
- Moore J, Grinsted A, Jevrejeva S (2006) Is there evidence for sunspot forcing of climate at multi-year and decadal periods? *Geophys Res Lett* 33(17):L17705
- Rossi A, Massei N, Laignel B, Sebag D, Copard Y (2009) The response of the Mississippi River to climate fluctuations and reservoir construction as indicated by wavelet analysis of streamflow and suspended-sediment load, 1950–1975. *J Hydrol* 377(3–4):237–244
- Schaeffli B, Maraun D, Holschneider M (2007) What drives high flow events in the Swiss Alps? Recent developments in wavelet spectral analysis and their application to hydrology. *Adv Water Resour* 30(12):2511–2525
- Smith LC, Turcotte DL, Isacks BL (1998) Stream discharge characterization and feature detection using a discrete wavelet transform. *Hydrol Process* 12:233–249
- Torrence C, Compo GP (1998) A practical guide to wavelet analysis. *Bull Am Meteorol Soc* 79(1):61–78
- Torrence C, Webster PJ (1999) Interdecadal changes in the ENSO-monsoon system. *J Climate* 12:2679–2690
- Yan Z, Zhou H, Liu W, Zhou L (2003) Preliminary discuss on grassland degradation in the source region of Yangtze and Yellow rivers. *Grassl China* 25:73–78 (in Chinese)
- Yang RW, Cao J, Huang W, Nian AB (2010) Cross wavelet analysis of the relationship between total solar irradiance and sunspot number. *Chin Sci Bull* 55(20):2126–2130
- Yellow River Commission (1999) ‘Some Basic Data of the Yellow River’, Huang-he Bao (The Yellow River Newspaper), October 1 (in Chinese)
- Zhang SF, Jia SF, Liu CM, Cao WB, Hao FH, Liu JY, Yan HY (2004) Study on the changes of water cycle and its impacts in the source region of the Yellow River. *Sci China Ser E* 47:142–151
- Zhang Y, Liu L, Bai W, Shen Z, Yan J, Ding M, Li S, Dong D (2006) Grassland degradation in the source region of the Yellow River. *Acta Geogr Sin* 61(1):3–14 (in Chinese)